DEVELOPMENT OF AN EQUATION-ORIENTED STEADY-STATE EVAPORATION PLANT SIMULATOR

Authors: Márcio R. Vianna Neto [1], Marcelo Cardoso [1], Esa K. Vakkilainen [2], Éder D. Oliveira [1]
[1] *Universidade Federal de Minas Gerais. Brazil*
[2] *Lappeenranta University of Technology. Finland*

ABSTRACT

An equation-oriented process simulator was developed for simulating evaporation plants. The simulator graphical user interface was written in Python 2.7, and its engine, in C++. The simulator orders and partitions the system of equations that describe the evaporator system under study and solves the partitions sequentially using the Newton-Raphson method. If no good initial estimates can be provided by the user, the simulator solves a simplified problem to generate the estimates, which greatly facilitates convergence. Calculations are based on steam table correlations and on black liquor enthalpy correlations described in the literature. Two multiple-effect counter-current evaporator scenarios were extracted from the literature and used to validate the simulator: a simple 3-effect system and a realistic 6-effect system. The simulator converged to the solutions with relative ease, provided that the model equations were written as described, that equations were ordered and partitioned, and the simplified model was used to generate good initial estimates. Good agreement was found between the calculated values and those reported in the literature, indicating that the proposed simulation framework could be extended to accommodate more complex systems. Deviations from the reported values can be explained by the different choices of physical properties correlations.

Keywords: *simulation, multiple-effect, evaporation, equation-oriented, partitioning*

1. INTRODUCTION

It is desirable to increase the energetic efficiency of pulping plants to make the process more competitive. Moreover, by increasing its energetic efficiency, less energy resources need to be consumed, lowering fossil-fired carbon dioxide generation, which is key to achieving sustainable development [1,2]. For these reasons, the energetic optimization of chemical pulping plants has received attention in the literature [3,4].

Black liquor is a residue produced during the chemical pulping process. In the chemical recovery cycle, black liquor is burned in the recovery boiler to produce energy and to recover chemicals that are consumed during the cooking process. This step is key to making the pulping process economically feasible [4, 5–7]. Before the black liquor can be burned in the recovery boiler, it is necessary to reduce its water fraction to increase combustion efficiency. Evaporation and drying are the most energy intensive steps in the chemical pulping process. Evaporation is typically carried out in a Multiple-Effect Evaporator (MEE) train, usually constituted of 5 to 7+ evaporator bodies. MEE trains concentrate black liquors from a dry solids mass fraction of approximately 15% to about 80-85% [8]. The evaporation step makes up 24-30% of the total energy used by a pulp mill, which justifies its optimization [9].

The simulation and optimization of MEE systems has received considerable attention in the literature. Cardoso *et al.* (2009) simulated and optimized a pulp mill for minimum energy consumption [6]. Saturnino (2012) modeled the chemical balance of a Kraft mill. The evaporator train was simulated using two commercial process simulators [7]. Ji *et al.* (2012) constructed a simplified evaporator model and conducted process integration through a mixed-integer linear programming (MILP) approach [4]. Mesfun and Toffolo (2013) applied a process integration methodology to optimize the evaporator train and the CHP system of a Kraft pulp and paper mill [3]. Several other deterministic and non-deterministic approaches to simulate MEE trains and optimize their energy consumption have also been tried [10–22]. Verma *et al.* (2019) recently published a review of methods used evaporator train simulation and optimization [19].

However, these approaches rely on the user having to hard code each individual system to be optimized, which is tedious and error-prone for large systems. In this paper we present an equation-oriented steady-state simulator constructed specifically to facilitate the optimization

Corresponding author: Márcio R. Vianna Neto. Universidade Federal de Minas Gerais. Av. Pres. Antônio Carlos, 6627 – Pampulha. Belo Horizonte – MG. 31270-901. Brazil. Phone: +55-31-34091735. marciorvneto@ufmg.br

of MEE systems. The equation-oriented architecture is advantageous for optimization because it exposes the equations that constitute the system under study, allowing their mathematical properties to be fully exploited. The simulator is general enough to enable systems of arbitrary complexity to be constructed, simulated and optimized. In this paper, we will focus on the architecture and validation of the results calculated by the simulator engine.

METHODS

Simulator architecture

The simulator is equation-oriented, which means that the unit processes involved in the simulation are abstracted as a system of equations, which is then solved. A *Graphical User Interface* (GUI) is exposed, through which it is possible to assemble the block diagram corresponding to the MEE system under study and to input process parameters. In these diagrams, unit processes are represented as blocks, which are interconnected through streams.

Figure 1 summarizes the calculation process carried out by the simulator. Initially, the user inputs a block diagram and its respective process parameters through the GUI. Blocks and streams, collectively referred in Figure 1 as *elements*, supply equations to the simulation engine, which assembles the *Global System of Equations* (GSE). The equations are then ordered to facilitate convergence.

The ordering process begins by constructing the bipartite graph corresponding to the GSE, as shown in [24]. In this graph, two sets of vertices exist: equation vertices and variable vertices. An edge connects an equation vertex i to a variable vertex j if variable j takes part in equation i. The maximum bipartite matching M for this graph is then determined using the Ford-Fulkerson algorithm. The bipartite graph is then converted into a directed graph through the following process: for every edge e connecting the equation vertex i to the variable vertex j, if e belongs to M, replace it by a directed edge connecting i to j. If e is not in M, replace it by a directed edge connecting j to i. The topological ordering of this directed graph gives the ordering of the equations.

Once the equations ordering has been determined, the simulator proceeds to determine the clusters of equations that need to be solved simultaneously. This step is referred to as partitioning the GSE.

Having completed these steps, the simulator solves each partition following the determined equation ordering using the Newton-Raphson (NR) method. Initial estimates for the variables may either be supplied by the user or asked to be calculated by the simulator. In the latter case, the simulator is run using simplified models for each unit process to facilitate convergence, as will be detailed in the next section. The values found by solving the simplified models are then used as initial estimates for the original system. The stopping criterion for NR is the Euclidean distance between two successive iterations, which must be smaller than some small error tolerance input by the user. Once the simulator has concluded its calculations, the results can be either displayed to the user via the GUI, or be fed to an objective function, if optimization is to be performed.

The GUI was developed using Python 2.7, whereas the graph algorithms, as well as the numerical routines were implemented in C++.

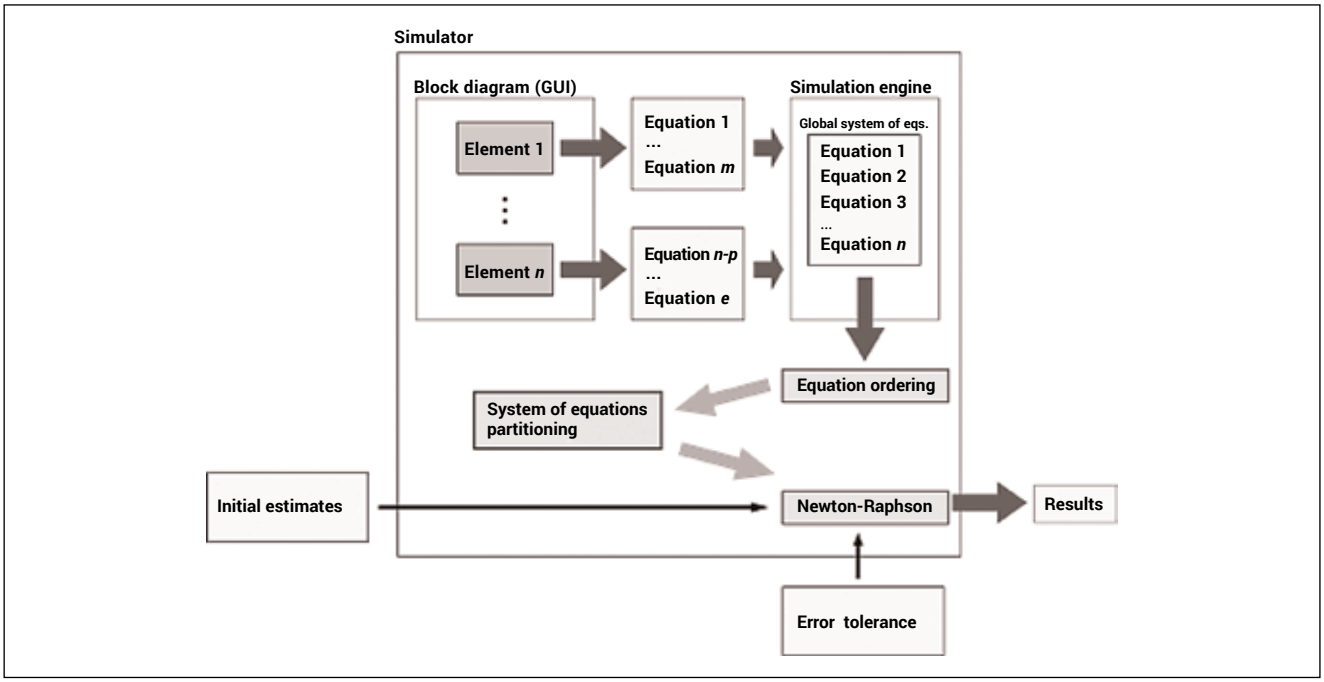

Figure 1. Simulator architecture

Table 1. Unit processes supported by the simulator and their respective equations.

Process block	Description	Equations
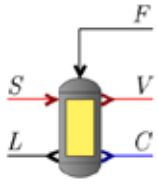 Evaporator	The black liquor stream F and the inlet vapor stream S enter the Evaporator block. The outlet black liquor stream L, the condensate stream C and the outlet vapor stream V exit the block. Evaporator blocks take as parameters the heat transfer coefficient U and the heat transfer area A.	$\dot{m}_S = \dot{m}_C$ $\dot{m}_F = \dot{m}_L + \dot{m}_V$ $\dot{m}_F x_{D,F} = \dot{m}_L x_{D,L}$ $P_S = P_C$ $T_C = T_{sat}(P_S)$ $T_V = T_{sat}(P_V) + BPR(P_V, x_{D,L})$ $T_V = T_L$ $Q = \dot{m}_S(H_S - H_C)$ $Q = UA(T_S - T_L)$ $\dot{Q} + \dot{m}_F H_F = \dot{m}_L H_L + \dot{m}_V H_V$
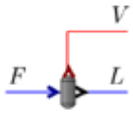 Flash tank	The inlet black liquor or condensate stream F enters the Flash block. The outlet vapor stream V and the outlet black liquor or condensate stream L exit the block. The flash tank pressure is determined by the outlet vapor stream pressure, P_V.	$\dot{m}_F = \dot{m}_L + \dot{m}_V$ $T_V = T_L$ $P_V = P_{sat}(T_V)$ $P_L = P_{sat}(T_V)$ $\dot{m}_F x_{D,F} = \dot{m}_L x_{D,L}$
 Black liquor mixer	An arbitrary number of black liquor streams L_i enter the mixer block, and a single combined black liquor stream L_{out} exits it.	$\sum \dot{m}_i = \dot{m}_{out}$ $\sum_i \dot{m}_i H_i = \dot{m}_{out} H_{out}$ $\sum_i \dot{m}_i x_{D,i} = \dot{m}_{out} x_{D,out}$
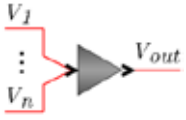 Vapor mixer	An arbitrary number of vapor or condensate streams V_i enter the mixer block, and a single combined vapor or condensate stream V_{out} exits it. In this work, the vapor mixer is assumed to cause negligible pressure drop and to impose that all pressures be equal.	$\sum \dot{m}_i = \dot{m}_{out}$ $\sum \dot{m}_i = \dot{m}_{out}$ $P_1 = P_2 = \ldots = P_n = P_{out}$

Unit processes, blocks and streams

The unit processes currently supported by the simulator are: evaporation, black liquor and condensate flashing, black liquor mixing, vapor and condensate mixing. Streams represent mass flows, and are divided into black liquor, vapor and condensate streams. Table 1 lists the currently supported process blocks and the equations corresponding to each of them. Table 2 lists the variables that describe each type of stream. In these equations, variable subscripts denote the streams to which they correspond, except the subscript *sat*, which denotes saturation. Mass flows are indicated by $\dot{m}$, enthalpies by H, temperatures and pressures by T and P respectively, the dissolved solids mass fraction by x_D and the boiling point rise of black liquor, by BPR.

As mentioned before, if no initial estimates are supplied by the user, the simulator solves simplified models to obtain those estimates. The simplified model equations are the same as those listed in Table 1, for all blocks, except the Evaporator. Its energy balance is replaced by the equation $\dot{m}_S = \dot{m}_V$ and the heat of steam condensation is approximated by $\dot{Q} = 2200 \cdot \dot{m}_S$.

Table 2. Stream types and their describing variables.

Stream type	Variables
Black liquor	$\dot{m}$, T, x_D
Vapor	$\dot{m}$, T, P
Condensate	$\dot{m}$, T, P

Physical properties

Energy balances require black liquor, water steam enthalpies to be known. Water and steam enthalpies were calculated from steam table correlations, implemented in C++ as described in the 2007 revised release on the *International Association for the Properties of Water and Steam* IAPWS Industrial Formulation of 1997 standard [25].

Black liquor enthalpies were calculated from the correlation described by Zaman and Fricke (1996), which expresses the enthalpy of black liquor at 80 °C, H_{80}, as shown in Equation (1) [26]. In this equation, H_w denotes the water enthalpy at 80 °C, x_D is the black liquor dissolved solids fraction, and the constants and depend on the type of black liquor being considered. In this work, it was assumed that *kJ/kg.K* and .

$$H_{80}=H_w+b\left[-1+exp\left(\frac{x_D}{c}\right)\right] \quad (1)$$

In order to account for black liquor enthalpies at other temperatures, H_{80} is corrected using the black liquor specific heat correlation given by Equation (2), where t stands for the temperature measured in °C [5].

$$c_p=4.216(1-x_D)+\left[1.675+\frac{3.31t}{1000.0}\right]x_D+\left[4.87+\frac{20t}{1000.0}\right](1-x_D)x_D^3 \quad (2)$$

The black liquor Boiling Point Rise (BPR) also needs to be considered in evaporator calculations. BPR is accounted for using Equations (3) and (4), where T_P is the boiling temperature of water at pressure P.

$$BPR(P,x_D)=BPR_{atm}(x_D)[1+0.6(T_P-373.16)/100] \quad (3)$$

$$BPR_{atm}(x_D)=6.173x_D-7.48x_D^{1.5}+32.747x_D^2 \quad (4)$$

Table 3. Input values for the 3-effect MEE system.

Variable	Value	Units
Live steam temperature	120	°C
Black liquor inlet mass flow	50	kg/s
Black liquor inlet temperature	70	°C
Black liquor inlet dissolved solids	20	%
Vapor temperature from E3	60	°C
Heat transfer coefficient of E1 (U1)	1.2	kW/m²K
Heat transfer coefficient of E2 (U2)	1.6	kW/m²K
Heat transfer coefficient of E2 (U3)	2.0	kW/m²K
Outlet black liquor dissolved solids	50	%

Validation scenarios

Two MEE plants were taken as case studies to validate the results given by the simulator. The first scenario was a simple counter-current 3-effect MEE system, depicted in Figure 2. In this scenario, condensate leaving the first and second effects are flashed and fed to the second and third effects, respectively. This system was adapted from [5] and, due to its relative simplicity, was intended to aid in the testing of the unit process models and the simulator code. Black streams denote black liquor, red streams denote vapor and blue streams, condensate.

The input values for this system are listed in Table 3. All heat exchange areas were assumed to be equal.

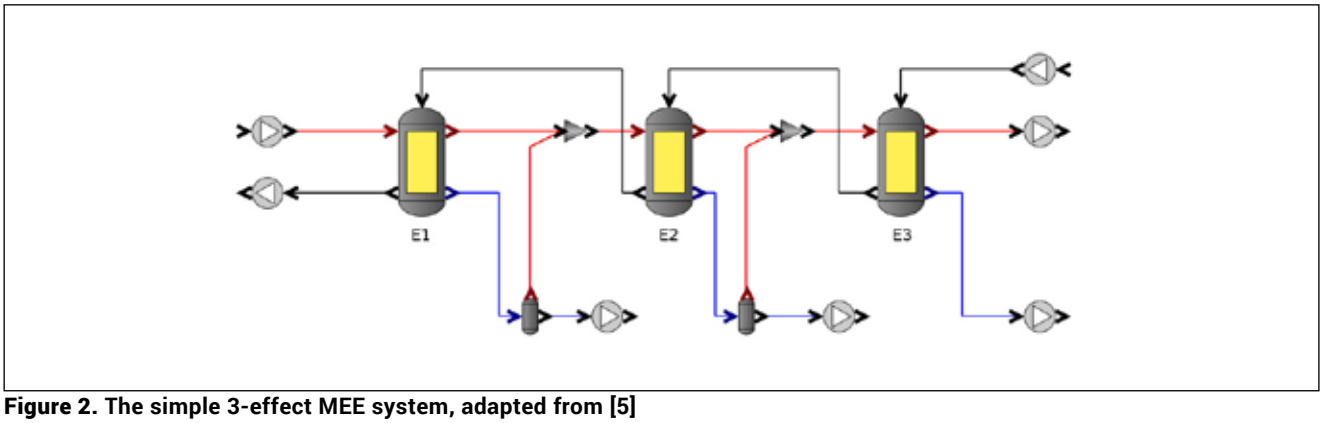

Figure 2. The simple 3-effect MEE system, adapted from [5]

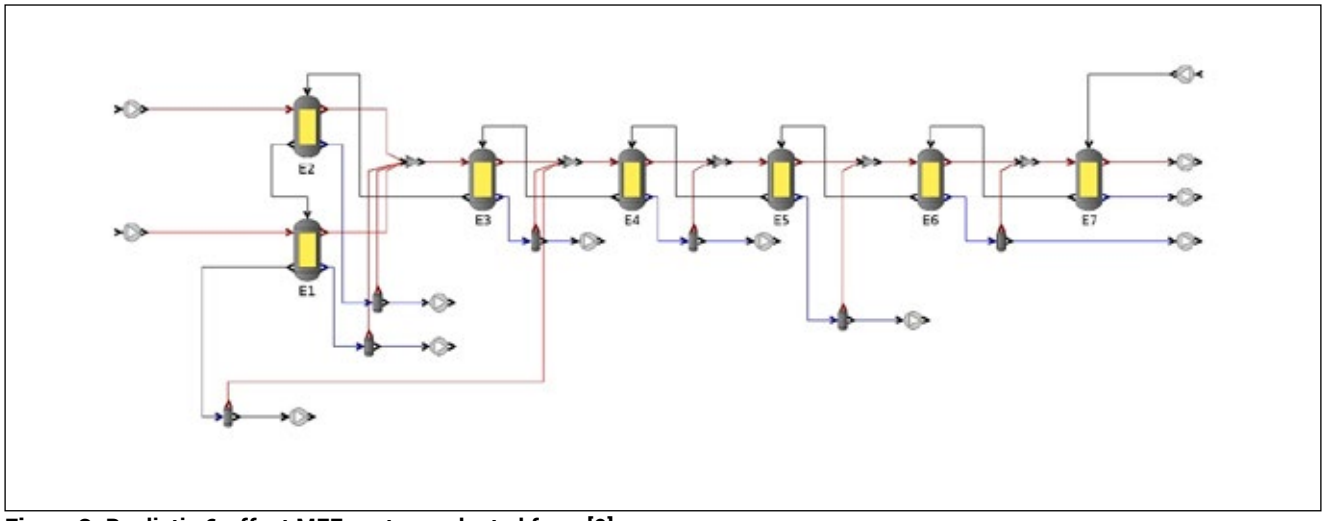

Figure 3. Realistic 6-effect MEE system, adapted from [9].

A more realistic 6-effect system was adapted from [9] and is shown in Figure 3. It should be noted that black liquor exiting the first effect is flashed and its vapor is fed to the fourth effect. In their original paper, Jyoti and Khanam (2014) used polynomial fits to estimate steam table properties and correlations to calculate the evaporators heat transfer coefficients. The input values for this system are listed in Table 4. All heat transfer areas were assumed to be equal.

Figure 2: Realistic 6-effect MEE system, adapted from [9].

The two systems were input to the simulator without supplying any initial estimates for the variables, which means that they were calculated by first solving the simplified models. The NR error tolerance was set to 10^{-6}.

Table 4. Input values for the 6-effect MEE system

Variable	Value	Units
Live steam temperature to E1	140	**°C**
Live steam temperature to E2	147	**°C**
Vapor temperature from E7	52	**°C**
Black liquor inlet mass flow	15.6	kg/s
Black liquor inlet temperature	64.7	**°C**
Black liquor inlet dissolved solids	11.8	%
Black liquor outlet dissolved solids	31	%
Heat transfer coefficient of E1 (U1)	0.296	kW/m²K
Heat transfer coefficient of E2 (U2)	0.4303	kW/m²K
Heat transfer coefficient of E2 (U3)	0.2584	kW/m²K
Heat transfer coefficient of E2 (U4)	0.6955	kW/m²K
Heat transfer coefficient of E2 (U5)	0.839	kW/m²K
Heat transfer coefficient of E2 (U6)	0.9698	kW/m²K
Heat transfer coefficient of E2 (U7)	1.224	kW/m²K

Table 5. Comparison between calculated values and reference values for the 3-effect system

Variable	Calculated value	Reference value	Units
Heat transfer areas (all effects)	810.0	1040.0	m^2
Vapor temperature from E1	93.7	91.6	°C
Vapor temperature from E2	74.2	73.3	°C
Vapor temperature from E3	60.0	60.0	°C
Black liquor dissolved solids from E1	50.0	50.0	%
Black liquor dissolved solids from E2	33.3	33	%
Black liquor dissolved solids from E3	25.2	25	%
Outlet black liquor temperature	93.7	99.8	°C
Live steam mass flow	11.6	11.3	kg/s

Table 6. Comparison between calculated values and reference values for the 6-effect system

Variable	Calculated value	Reference value	Units
Vapor temperature from E1	129,0	106,3	°C
Vapor temperature from E2	128,5	126,8	°C
Vapor temperature from E3	93,6	89,5	°C
Vapor temperature from E4	78,3	77,2	°C
Vapor temperature from E5	67,1	67,2	°C
Vapor temperature from E6	58,3	58,7	°C
Vapor temperature from E7	52,0	52	°C
Black liquor dissolved solids from E1	29.17	31.65	%
Black liquor dissolved solids from E2	26.59	26.29	%
Black liquor dissolved solids from E3	23.08	24.42	%
Black liquor dissolved solids from E4	19.59	20.32	%
Black liquor dissolved solids from E5	16.66	17.29	%
Black liquor dissolved solids from E6	14.67	15.12	%
Black liquor dissolved solids from E7	13.24	13.45	%
Total live steam mass flow	2.2	1.9	kg/s

RESULTS AND DISCUSSION

Table 5 displays some of the key variables found for the 3-effect MEE system, and their respective values as reported from the original reference. Notice that there is a strong agreement between calculated and reference values. There is, however, the simulator underestimated the heat transfer area and the black liquor outlet temperature, as compared to the reference values. This discrepancy is justified by the fact that the black liquor enthalpies in this work were calculated from different correlations than those of the original reference.

Table 6 displays some of the key variables found for the 6-effect MEE system, and their respective values as reported from the original reference. As before, there is a strong agreement between calculated and reference values, and the discrepancy are likely due to the different correlations used. Notice that the heat transfer areas are not shown in Table 6, as they were not reported in the original publication.

It should be noted that the steps of ordering the GSE, partitioning it and obtaining initial estimates by solving the simplified model were critical to ensure that the simulator would converge. In both scenarios, the combination of these steps allowed the simulator to converge with relative ease. This, however, was not the case when any of the steps were skipped. Solving all the equations simultaneously via NR proved to be a particularly poor approach, as poor initial estimates often led to singular Jacobians during the NR iterations.

It must also be emphasized that the simulator determines the ordering of the GSE based on the form taken by each equation

i.e. the set of variables present in each equation. In other words, the way the equations are written has a direct impact on the performance of the simulator. The equations described in Table 1 are written in the way that yielded the most satisfactory results.

CONCLUSIONS

The simulator was capable of calculating realistic MEE systems. To facilitate convergence, it is desirable to make sure that the equations take a suitable form and that they are ordered and partitioned. If no good initial estimates can be given, it is also desirable to solve a simplified model to generate reasonable estimates.

The simulator currently assumes that the heat transfer coefficient is given by the user, as opposed to being calculated by the simulator. In the future, this issue may be addressed by introducing heat transfer correlations. In future work, more unit processes can be modeled, such as condensate preheaters and recovery boilers, which would allow for more realistic scenarios to be simulated. More complex systems should also be tested to verify if the current solution strategy remains robust.

ACKNOWLEDGEMENTS

The authors are indebted to the Conselho Nacional de Desenvolvimento Científico e Tecnológico (CNPq/BRAZIL) and Fundação de Amparo à Pesquisa do Estado de Minas Gerais (Fapemig/BRAZIL) for supporting this study. ■

REFERENCES

1. T. Fleiter, D. Fehrenbach, E. Worrell, and W. Eichhammer, "Energy efficiency in the German pulp and paper industry–A model-based assessment of saving potentials," Energy, vol. 40, no. 1, pp. 84–99. (2012).
2. L. Kong, A. Hasanbeigi, and L. Price, "Assessment of emerging energy-efficiency technologies for the pulp and paper industry: a technical review," Journal of Cleaner Production, vol. 122, pp. 5–28. (2016).
3. S. Mesfun and A. Toffolo, "Optimization of process integration in a Kraft pulp and paper mill–Evaporation train and CHP system," Applied energy, vol. 107, pp. 98–110. (2013).
4. X. Ji, J. Lundgren, C. Wang, J. Dahl, and C.-E. Grip, "Simulation and energy optimization of a pulp and paper mill–Evaporation plant and digester," Applied energy, vol. 97, pp. 30–37. (2012).
5. P. Tikka, "Chemical pulping part 2, Recovery of chemicals and energy," Papermaking Science and Technology. (2008).
6. M. Cardoso, K. D. de Oliveira, G. A. A. Costa, and M. L. Passos, "Chemical process simulation for minimizing energy consumption in pulp mills," Applied Energy, vol. 86, no. 1, pp. 45–51. (2009).
7. D. M. Saturnino, Modeling of kraft mill chemical balance. PhD thesis, University of Toronto. (2012).
8. M. R. Olsson, Simulations of Evaporation Plants in Kraft Pulp Mills: Including Lignin Extraction and Use of Excess Heat. PhD thesis, Chalmers University of Technology. (2009).
9. G. Jyoti and S. Khanam, "Simulation of heat integrated multiple effect evaporator system," International Journal of Thermal Sciences, vol. 76, pp. 110–117. (2014).
10. R. Bhargava, S. Khanam, B. Mohanty, and A. Ray, "Selection of optimal feed flow sequence for a multiple effect evaporator system," Computers & Chemical Engineering, vol. 32, no. 10, pp. 2203–2216. (2008).
11. X. Ding, W. Cai, L. Jia, and C. Wen, "Evaporator modeling–A hybrid approach," Applied Energy, vol. 86, no. 1, pp. 81–88. (2009).
12. M. Sagharichiha, A. Jafarian, M. Asgari, and R. Kouhikamali, "Simulation of a forward feed multiple effect desalinationplant with vertical tube evaporators," Chemical Engineering and Processing: Process Intensification, vol. 75, pp. 110–118. (2014).
13. M. Kermani, Z. Périn-Levasseur, M. Benali, L. Savulescu, and F. Maréchal, "A novel MILP approach for simultaneous optimization of water and energy: Application to a Canadian softwood Kraft pulping mill," Computers & Chemical Engineering, vol. 102, pp. 238–257. (2017).
14. C. Diel, R. Canevesi, D. Zempulski, J. Awadallak, C. Borba, F. Palú, and E. Silva, "Optimization of multiple-effect evaporation in the pulp and paper industry using response surface methodology," Applied Thermal Engineering, vol. 95, pp. 18–23. (2016).
15. S. Khanam and B. Mohanty, "Development of a new model for multiple effect evaporator system," Computers & Chemical Engineering, vol. 35, no. 10, pp. 1983–1993. (2011).
16. O. P. Verma, G. Manik, and T. H. Mohammed, "Energy management in multi stage evaporator through a steady and dynamic state analysis," Korean Journal of Chemical Engineering, vol. 34, no. 10, pp. 2570–2583. (2017).
17. O. P. Verma, G. Manik, V. K. Jain, D. K. Jain, H. Wang, et al., "Minimization of energy consumption in multiple stage evaporator using genetic algorithm," Sustainable Computing: Informatics and Systems, vol. 20, pp. 130–140. (2018).
18. O. P. Verma, T. H. Mohammed, S. Mangal, and G. Manik, "Minimization of energy consumption in multi-stage evaporator system of kraft recovery process using interior-point method," Energy, vol. 129, pp. 148–157. (2017).
19. O. P. Verma, G. Manik, and S. K. Sethi, "A comprehensive review of renewable energy source on energy optimization of black liquor in MSE using steady and dynamic state modeling, simulation and control," Renewable and Sustainable Energy Reviews, vol. 100, pp. 90–109. (2019).
20. M. Khademi, M. Rahimpour, and A. Jahanmiri, "Simulation and optimization of a six-effect evaporator in a desalination process," Chemical Engineering and Processing: Process Intensification, vol. 48, no. 1, pp. 339–347. (2009).
21. D. Srivastava, B. Mohanty, and R. Bhargava, "Modeling and simulation of mee system used in the sugar industry," Chemical engineering communications, vol. 200, no. 8, pp. 1089–1101. (2013).
22. S. Khanam and B. Mohanty, "Energy reduction schemes for multiple effect evaporator systems," Applied Energy, vol. 87, no. 4, pp. 1102–1111. (2010).
23. D. Kaya and H. I. Sarac, "Mathematical modeling of multiple-effect evaporators and energy economy," Energy, vol. 32, no. 8, pp. 1536–1542. (2007).
24. Fritzson, P. "Principles of object-oriented modeling and simulation with Modelica 2.1.". John Wiley & Sons. (2010).
25. W. Wagner and H.-J. Kretzschmar, International Steam Tables-Properties of Water and Steam based on the Industrial Formulation IAPWS-IF97: Tables, Algorithms, Diagrams, and CD-ROM Electronic Steam Tables-All of the equations of IAPWS-IF97 including a complete set of supplementary backward equations for fast calculations of heat cycles, boilers, and steam turbines. Springer Science & Business Media. (2007).
26. A. Zaman and A. Fricke, "Heat of dilution and enthalpy concentration relations for slash pine kraft black liquors," Chemical Engineering Communications, vol. 155, no. 1, pp. 197–216. (1996).